An *ab initio* study of magneto-electric coupling of $YMnO_3$

2013 J. Phys.: Condens. Matter 25 496004

(http://iopscience.iop.org/0953-8984/25/49/496004)

J. Phys.: Condens. Matter **25** (2013) 496004 (7pp) doi:10.1088/0953-8984/25/49/496004

An *ab initio* study of magneto-electric coupling of $YMnO_3$

J Varignon[1], S Petit[1], A Gellé[2] and M B Lepetit[3,4,5]

[1] CRISMAT, ENSICAEN-CNRS UMR 6508, 6 Boulevard Maréchal Juin, 14050 Caen, France
[2] Institut de Physique de Rennes, UMR CNRS 6251, Université Rennes 1, 263 Avenue Général Leclerc, 35042 Rennes, France
[3] Institut Néel, UPR-2940 CNRS, 25 rue des Martyrs BP 166, 38042 Grenoble cedex 9, France
[4] Institut Laue Langevin, BP 156, 6, rue Jules Horowitz, 38042 Grenoble cedex 9, France

E-mail: Marie-Bernadette.Lepetit@Grenoble.cnrs.fr

Received 26 July 2013, in final form 27 September 2013
Published 6 November 2013
Online at stacks.iop.org/JPhysCM/25/496004

Abstract
This paper proposes the direct calculation of the microscopic contributions to the magneto-electric coupling, using *ab initio* methods. The electrostrictive and the Dzyaloshinskii–Moriya contributions were evaluated individually. For this purpose a specific method was designed, combining density functional theory calculations and embedded fragment, explicitly correlated, quantum chemical calculations. This method allowed us to calculate the evolution of the magnetic couplings as a function of an applied electric field. We found that in $YMnO_3$ the Dzyaloshinskii–Moriya contribution to the magneto-electric effect is three orders of magnitude weaker than the electrostrictive contribution. Strictive effects are thus dominant in the magnetic exchange evolution under an applied electric field, and by extension in the magneto-electric effect. These effects however, remain quite small, and the modifications of the magnetic excitations under an applied electric field will be difficult to observe experimentally. Another important conclusion is that it can be shown that the linear magneto-electric tensor is null due to the inter-layer symmetry operations.

(Some figures may appear in colour only in the online journal)

1. Introduction

Multiferroic materials have been known since the work of Curie in 1894 [1], and of Bauer in 1926 [2]. During recent years they have received increased attention due to the discovery of colossal magneto-electric effects [3]. In such systems, the magnetic properties (magnetization, magnetic ground state, etc) can be controlled using an electric field, and the electric properties (polarization, dielectric constant, etc) can be controlled using a magnetic field. In spite of the multiple studies done over the years, the microscopic origin of the magneto-electric coupling is still relatively unknown. While the spin–orbit coupling is the only term in the Hamiltonian that couples the magnetic degrees of freedom with the charge degrees of freedom, other effects such as electrostrictive/magnetostrictive indirect coupling have also been proposed as candidates for the origin of the magneto-electric coupling. The aim of this paper will thus be to directly compute the different microscopic mechanisms contributing to the magneto-electric effect.

Multiferroic systems are generally classified into type I and type II compounds. Type I materials are characterized by a paraelectric/ferroelectric transition distinct from the magnetic transition, while for type II systems ferroelectricity appears at a magnetic transition. In this paper, we will focus on one of the most typical type I materials, $YMnO_3$. This compound exhibits a paraelectric/ferroelectric transition at high temperature (with the appearance of a spontaneous polarization along the **c** axis), and an antiferromagnetic transition at 74 K. A magneto-electric coupling in the low temperature phase has been evidenced by several groups [4] through the apparition of an anomaly in the dielectric constant at the Néel temperature. This magneto-electric coupling was first explained by Goltsev *et al* [5] as a piezomagnetic

[5] Previously at CRISMAT, CNRS-ENSICAEN, Caen, France.

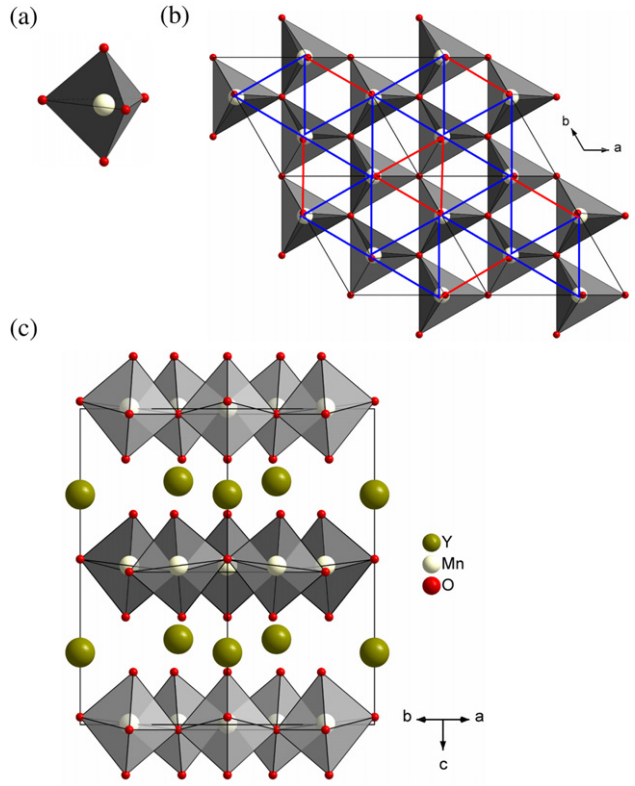

Figure 1. Structure of the $YMnO_3$ compound. (a) MnO_5 bipyramid. (b) Two-dimensional triangular layers of MnO_5 bipyramids; the two types of Mn–Mn bond are respectively underlined in blue and red. (c) Complete crystal structure.

interaction between ferroelectric and antiferromagnetic domain walls. Then Hanamura *et al* [6] proposed a spin–orbit origin, through a dependence of the exchange integrals on the polarization sign. Finally, Lee *et al* [7] proposed an electrostrictive/magnetostrictive microscopic origin. $YMnO_3$ thus looks like a good candidate for a theoretical investigation on the origin of the magneto-electric coupling. In addition, it presents the advantage to display only one magnetic species, the manganese ions.

$YMnO_3$ crystallizes in a hexagonal structure, in the $P6_3cm$ space group under the paraelectric/ferroelectric transition. The structure is based on corner-sharing MnO_5 bipyramids, organized in two-dimensional triangular layers (see figure 1). The yttrium atoms are located in between the bipyramid layers. The triangular arrangement of the manganese atoms is not ideal and there are two different types of Mn–Mn bonds (see figure 1(b)). Structurally, the antiferromagnetic transition is seen as an isostructural $P6_3cm$ to $P6_3cm$ one. This transition is however associated with large atomic displacements [7], strongly affecting the polarization amplitude [8, 9]. The associated magnetic order was long believed to belong to the totally symmetric irreducible representation of the $P6_3cm$ magnetic group [10]; however, it was recently shown that the magnetic group can only be $P6'_3$, losing the symmetry planes orthogonal to the layers [9, 11].

The magnetism is due to the Mn^{3+} manganese ions ($3d^4$) in a high spin state ($S = 2$). The trigonal symmetry of the bipyramids splits the 3d orbitals as pictured in figure 2, leaving an empty $3d_{z^2}$ orbital. The resulting atomic spins form a triangular lattice with frustrated antiferromagnetic interactions. Neutron scattering experiments show in-plane orientation of the manganese spins with a 120° arrangement [10]. However, more recently, a very weak ferromagnetic component, oriented along the **c** axis, has been observed and shown to be due to the spin–orbit coupling [9]. At this point let us note that the spin–orbit interaction (as well as the Dzyaloshinskii–Moriya effective model) breaks the $P6_3cm$ symmetry group and induces a lowering of the symmetry to the $P6'_3$ magnetic group and associated $P6_3$ crystallographic group.

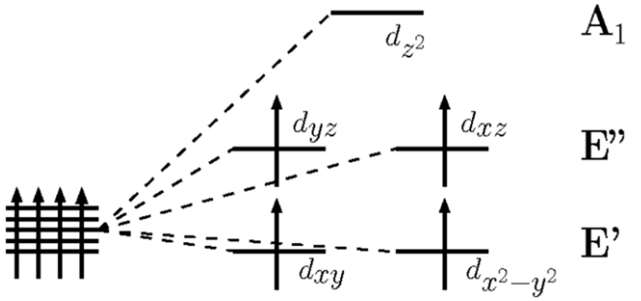

Figure 2. Splitting of the 3d orbitals for the Mn^{3+} ions.

The present paper will be organized as follows. Section 2 will be devoted to the presentation of the method used for the calculation of the magneto-electric coupling. Section 3 will present the results on the exchange integrals while section 4 will present the results on the magneto-electric coupling. Finally, the last section will propose a conclusion.

2. Computing the microscopic contributions to the magneto-electric effect

How to compute the microscopic contributions to the magneto-electric effect? One possibility would be to compute the electric properties (polarization, dielectric constant, etc) as a function of an applied magnetic field. This is the line followed by some authors, applying a Zeeman field within a density functional calculation [12]. Another possibility is to compute the magnetic state as a function of an applied electric field. In this work, we chose to use the second method. Indeed, the polarization or dielectric constant can only be computed using density functional theory (DFT) or related mean-field methods (see for instance [13]). However, such methods encounter difficulties in accurately evaluating the magnetic couplings, crucial for the magneto-electric effect. For instance, in the present system, even when using the hybrid B3LYP functional, DFT calculations of the exchange integral yield −0.59 meV [14], to be compared with the −2.3 meV [15] and −3 meV [16] evaluations from inelastic neutron scattering, and with the −2.7 meV [14] evaluation found using the fully correlated wavefunction SAS + S method used in the present work (see below for details). We will thus compute, using the SAS + S *ab initio* method (with and without spin–orbit interactions), the magnetic coupling constants as a function of an applied electric field. These integrals can in a second step be used

within the underlying effective magnetic Hamiltonian: the Heisenberg model, corrected by the Dzyaloshinskii–Moriya interaction [17], on a two-dimensional triangular lattice.

$$H = -\sum_{\langle i,j\rangle} J_{ij}\,\vec{S}_i \cdot \vec{S}_j + \vec{D}_{ij} \cdot \vec{S}_i \wedge \vec{S}_j \qquad (1)$$

where the sum over $\langle i, j\rangle$ runs over all Mn–Mn nearest neighbor bonds. The *ab initio* parameterized model can then be used to derive the magneto-electric coupling tensor.

The next question is 'what is the main effect of an applied electric field?'. According to Iñiguez [18], the main effect is the nuclear displacements induced by the electric field. Indeed, most of the time, the external field is efficiently screened and the orbital polarization due to the applied field can be neglected [12, 18]. Since an electric field does not directly couple to spins, the spin contribution (important when a magnetic field is applied) only comes through the spin–orbit term. When the spin–orbit coupling and orbital moment remain small (as in the present system, see below) so will be the orbital polarization. Of course this would not be the case in systems where the spin–orbit coupling is rather large [19]. The atomic displacements $\vec{d}$ can be determined using Newton's second law as

$$\overline{\overline{Z}}^{\star} \cdot \vec{E} = \overline{\overline{\mathcal{H}}} \cdot \vec{d} \qquad \Leftrightarrow \qquad \vec{d} = \overline{\overline{\mathcal{H}}}^{-1} \cdot \overline{\overline{Z}}^{\star} \cdot \vec{E} \qquad (2)$$

where $\vec{E}$ is the applied electric field, $\overline{\overline{Z}}^{\star}$ is the Born charge tensor, $\overline{\overline{\mathcal{H}}}$ is the Hessian matrix of the electronic Hamiltonian and $\vec{d}$ is the sought displacement vector.

Our aim is to compute the magnetic exchange integrals under such displacements. However, there is no theoretical technique able to simultaneously give, with reliable accuracy, the elastic effects and the magnetic integrals. Indeed, while the former are induced by the system as a whole (infinite and total electronic density) and have little dependence on the Fermi electrons (they account for only a small part of the total energy), the latter are essentially local and dominated by the physics of the Fermi level strongly correlated electrons. An accurate evaluation of the magnetic integrals requires a thorough treatment of the electron correlation. We thus developed a two-step approach, combining density functional (DFT) calculations for the elastic part and quantum chemical embedded fragment calculations for the magnetic part. The first step consists of the calculation of the Hessian matrix and the Born effective charge tensor using DFT. The atomic displacements induced by an applied electric field are then evaluated using equation (2). The second step consists in computing the magnetic exchange integrals associated with the new geometries. For this purpose, we used the SAS + S method [14] that was specifically designed for the accurate evaluation of magnetic excitations, in strongly correlated systems with numerous open shells per atom. The SAS + S method is a configuration interaction method (exact diagonalization within a selected configuration space) explicitly including the correlation within the metal d shells, the ligand-to-metal charge transfers, and the screening effects on both phenomena. It allows an accurate calculation of low energy excitation spectra as magnetic excitations. This method can however only be applied to finite systems. Appropriate embedded fragments were thus designed. In the present work the fragments were built from two Mn ions and their first coordination shells for the quantum part (see figure 3). Indeed, it has been shown by different groups [20] that the magnetic exchanges are local (the only important nonlocal effect is the Madelung potential, that, in the present work, was taken into account through the embedding, see below) and that the enlargement of the fragment, further than the first coordination shell of the magnetic atoms, does not modify in any significant manner the evaluation of the effective magnetic exchanges. These quantum fragments were embedded in an environment reproducing the main effects of the rest of the crystal: (i) the exclusion effects of the surrounding electrons and (ii) the long range Madelung potential. The former were modeled using total ion pseudopotentials [21] at surrounding atomic positions. The latter was computed using a set of point charges, located at atomic positions. These charges were renormalized on the external part, following the scheme described in [22], so as to ensure an exponential converge of the Madelung potential.

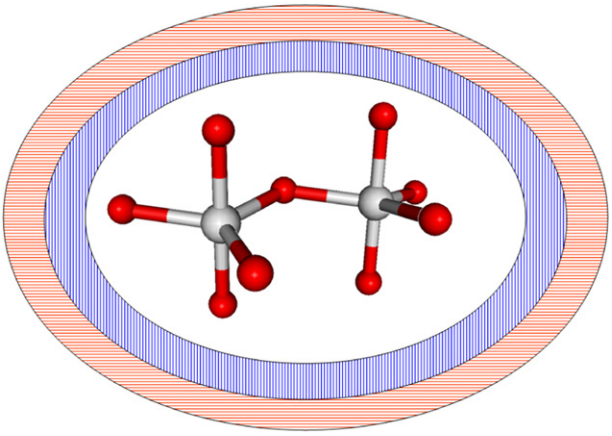

Figure 3. Schematic representation of the embedded clusters. The quantum part is explicitly shown, the vertically dashed (blue) surrounding part represents the total ion pseudopotentials (two shells of neighboring atoms), while the horizontally dashed (red) part represents the point charges (∼66 000 renormalized point charges).

In order to differentiate the relative importance of the different mechanisms responsible for the magneto-electric coupling, we computed the embedded cluster magnetic spectrum, as a function of an applied electric field, with and without the spin–orbit interaction.

Technical details. The DFT calculations were performed using the CRYSTAL09 package [23]. Since the manganese 3d shells are strongly correlated we used the hybrid B1PW [24] functional (hybrid functional specifically derived for the treatment of ferroelectric compounds) in order to better take into account the self-interaction cancellation. Small core pseudopotentials were used for the heavy atoms (Mn and Y) associated with semi-valence and valence 2ζ and 2ζ plus polarization basis sets [25]. The oxygen ions were represented in an all-electron basis set of 2ζ quality specifically optimized

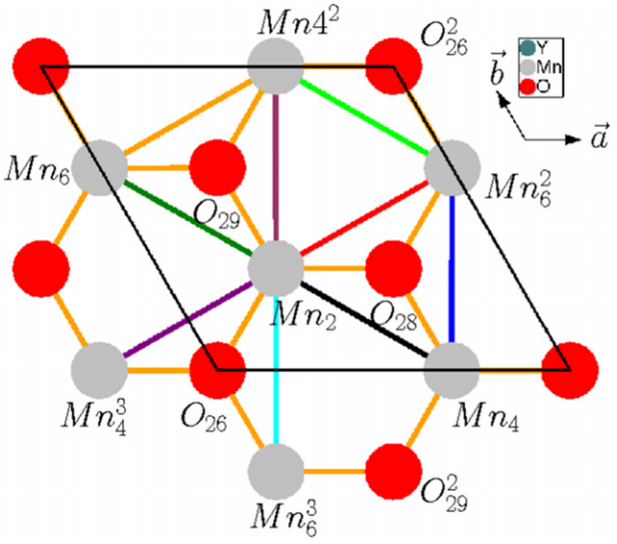

Figure 4. Representation of the nine magnetic interactions induced by the application of an electric field in the (**a**, **b**) plane.

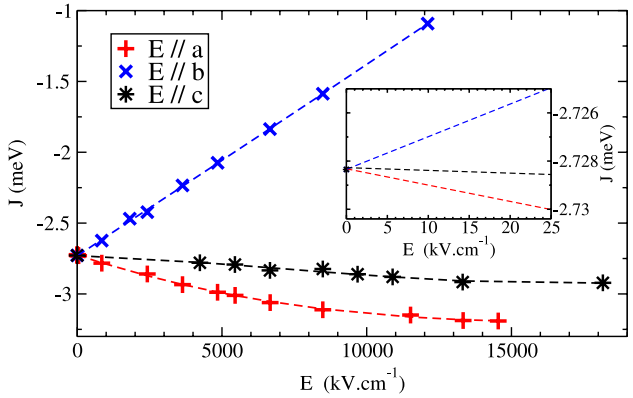

Figure 5. Evolution of the exchange integral (Mn_2–O_{28}–Mn_6^2 bond) as a function of an applied electric field along the **a**, **b** and **c** directions. The inset details the part of the curves associated with experimentally accessible electric fields.

for O^{2-} ions [25]. This method was used with great success in a previous work to compute the phonon spectrum, whose agreement with experimental observations guarantees its quality. For the details, see [26]. The SAS + S method was successively performed using the MOLCAS [27] package for the integrals and the fragment orbital calculations, the CASDI package for the configuration interaction, and the EPCISO [28] package for the spin–orbit calculations. A 3-ζ valence basis and core pseudopotential set was used in the calculation [29].

3. Results: the exchange integrals in the $YMnO_3$ compound

The magnetic exchange integrals are computed from the excitation energies between the $S = 4$ and 3 states of the embedded fragments. Indeed in a Heisenberg picture, the excitation energy between these states is associated with $4J$.

In the $YMnO_3$ compound, there are two independent magnetic integrals, associated with the two previously mentioned Mn–Mn types of bond (see figure 1(b)). We computed the magnetic integrals associated with the short Mn–Mn bonds, $J_s = -2.73$ meV, and the long Mn–Mn bonds, $J_l = -2.47$ meV. These values compare well with the evaluations obtained from the fitting of inelastic neutron scattering on a homogeneous triangular model: $J = -2.3$ meV [15] and $J = -3$ meV [16], thus validating the quality of the SAS + S method.

4. Results: the magneto-electric coupling

The application of an electric field in the (**a**, **b**) plane destroys the point symmetries and increases the number of non-equivalent magnetic integrals from two to nine (see figure 4).

4.1. Without the spin–orbit interaction

We first focused on one of the Mn–Mn bonds, and studied the evolution of its magnetic coupling as a function of an applied electric field in the three crystallographic directions. The bond under consideration is the short bond referred to as Mn_2–O_{28}–Mn_6^2 and pictured in red in figure 4—Mn atoms are located at (x_{Mn}, x_{Mn}, $z_{Mn}+1/2$) and at (1, $1-x_{Mn}$, $z_{Mn}+1/2$). The results are displayed in figure 5. When the electric field is applied along the **c** direction, the magnetic coupling remains essentially unchanged. When the electric field is applied along the **b** direction, that is perpendicular to the Mn–Mn bond axis, the exchange integral is strongly affected by the field and its antiferromagnetic character is reduced. Its behavior is essentially linear as a function of the electric field E with $J = -2.73 + 1.36 \times 10^{-4}\ E$. When the field is along the **a** direction, the Mn–Mn bond presents an angle of 30° with the field direction. In this case the antiferromagnetic character of the exchange integral is slightly increased. Figure 6 portrays the atomic displacements when the field is applied along the three directions. The J behavior as a function of the electric field direction can be understood considering these induced displacements on direct and super-exchange terms. When the field is along the **c** direction the Mn and O planes are closing in, increasing the antiferromagnetic character. This increase remains very small since the Mn and O planes are already very close (~0.2 Å) and the super-exchange term varies as $1 - \alpha h^2$ where h is the inter-plane distance. Second, the Mn–O–Mn angle is slightly opening up, decreasing the antiferromagnetic character. As a result, the electric field has little effect. When the field is along the **b** direction, the main effect is to increase the Mn–O bond lengths, and thus to reduce the magnetic-to-ligand orbital overlap, responsible for the super-exchange mechanism. As a result, the antiferromagnetic character is strongly reduced. Finally, when the field is applied along the **a** direction, one of the Mn–O distances is reduced, while the other one is increased, the Mn–Mn distance remaining unchanged. This mechanism results in an opening of the Mn–O–Mn angle. While the effects of the distance changes compensate each other, the Mn–O–Mn angle

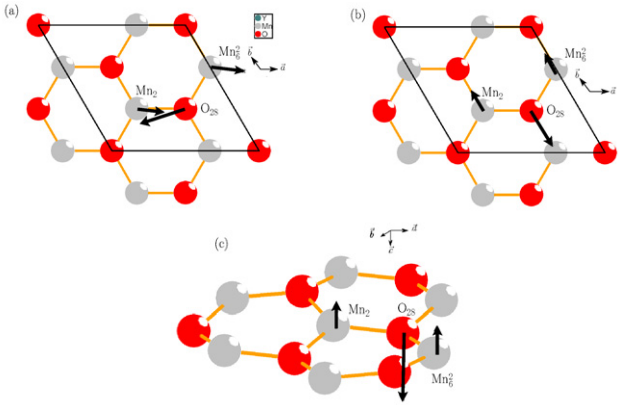

Figure 6. Atomic displacements for an applied electric field along the (a) **a** direction, (b) **b** direction and (c) **c** direction. For experimentally accessible fields the displacements are negligible. For instance, for an applied field of 10 kV cm^{-1} along the **a** direction one gets $\delta d_{\text{Mn–Mn}} = -1 \times 10^{-9}$ Å, $\delta d_{\text{Mn–O}} = -1.7 \times 10^{-6}$ and 0.7×10^{-6} Å, $\delta\widehat{\text{Mn–O–Mn}} = 5 \times 10^{-5}$°. For an applied field of ∼50 kV cm^{-1} one gets along the **a** direction $\delta d_{\text{Mn–Mn}} = 7 \times 10^{-4}$ Å, $\delta d_{\text{Mn–O}} = -6 \times 10^{-2}$ and 3×10^{-2} Å, $\delta\widehat{\text{Mn–O–Mn}} = 1.3$°; along the **b** direction $\delta d_{\text{Mn–Mn}} = 3 \times 10^{-4}$ Å, $\delta d_{\text{Mn–O}} = 3 \times 10^{-2}$ Å, $\delta\widehat{\text{Mn–O–Mn}} = -2.6$°; and along the **c** direction $\delta d_{\text{Mn–Mn}} = -2 \times 10^{-3}$ Å, $\delta d_{\text{Mn–O}} = -4 \times 10^{-3}$ Å, $\delta\widehat{\text{Mn–O–Mn}} = 0.3$°.

opening increases the metal-to-ligand orbital overlap, thus increasing the super-exchange antiferromagnetic contribution. Let us now concentrate on experimentally accessible electric field values (see inset of figure 5); one should notice that, even for fields as large as 10 kV cm^{-1}, the renormalization of the magnetic coupling remains very small, at most of the order 10^{-3} meV. One should thus unfortunately conclude that the effect of an electric field on the $YMnO_3$ magnetic spectrum should be experimentally difficult to observe.

Due to the hexagonal symmetry of $YMnO_3$, applying the field along the **a** or **b** directions is equivalent by symmetry on the whole system. We will thus compute the nine different exchange integrals with the field applied along the **a** direction. Figure 7 displays the results for the nine dimers. One sees that there are only two behaviors, corresponding to the field perpendicular to the Mn–Mn bonds and to the field at 30° with the Mn–Mn bonds. For each behavior, the two sets of curves are associated with the two types of Mn–Mn bond in zero field.

4.2. With the spin–orbit interaction

We then computed the spin–orbit correction on the embedded fragment magnetic spectrum, using the *ab initio* wavefunction EPCISO code from the Lille group [28]. As implicitly done in the previous section (where the *ab initio* results were mapped into an effective Heisenberg model), we will map the *ab initio* spin–orbit correction onto an effective Dzyaloshinskii–Moriya model ($\vec{D} \cdot (\vec{S}_i \wedge \vec{S}_j)$). Following the calculation done by Moriya on a single electron system [17], one can show that the ground state corrections due to the spin–orbit coupling for our four electrons per site system can

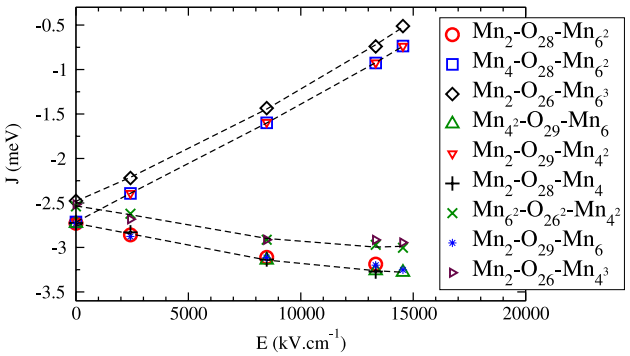

Figure 7. Evolution of the nine different magnetic couplings under an applied electric field along the **a** direction.

Table 1. Dzyaloshinskii–Moriya vector $\vec{D}$ as a function of an applied electric field. $\vec{D}$ was extracted from *ab initio* wavefunction calculations for a few representative values of the field amplitude.

Field direction	Field amplitude (kV cm^{-1})	D_{ab} (meV)	D_c (meV)
—	0	0.000 58	0.003 83
a	36 359	0.000 69	0.004 65
a	145 436	0.001 21	0.008 41
a	181 795	0.001 51	0.010 01
b	48 479	0.000 37	0.001 93
b	181 795	0.001 69	0.003 28
c	84 838	0.000 53	0.004 03
c	109 077	0.000 54	0.004 14

also be mapped onto a Dzyaloshinskii–Moriya model. The latter yields

$$\begin{aligned}\hat{H}_{\text{DM}}\Psi_{\text{GS}} = {} & (D_y + \mathrm{i}D_x)\Psi_{S=1,S_z=1} \\ & - (D_y - \mathrm{i}D_x)\Psi_{S=1,S_z=-1} \\ & - \mathrm{i}D_c\sqrt{2}\Psi_{S=1,S_z=0}\end{aligned}$$

where D_x and D_y correspond to the in-plane components of the Dzyaloshinskii–Moriya prefactor and D_c to its out-of-plane component. At this point let us note that, assuming purely atomic magnetic orbitals, and second order perturbation in the spin–orbit operator, the component on $\Psi_{S=1,S_z=0}$ should be zero, and thus so should be D_c. Similarly, under this hypothesis $D_x = D_y = D_{ab}$. The D_{ab} and D_c amplitudes can be extracted from *ab initio* calculations as the spin–orbit Hamiltonian matrix terms expressed on the *ab initio* spin-only states. Results for a few representative points are displayed in table 1.

One can see immediately that the Dzyaloshinskii–Moriya interaction remains extremely small in this system, with an order of magnitude 10^2–10^3 weaker than the exchange part. Its modulation as a function of the field is only a few 10^{-3} meV.

The exchange-striction contributions are thus much larger than the spin–orbit ones. These direct, quantitative calculations confirm the conclusions found by indirect methods such as (i) the fact that DFT evaluation of the spontaneous polarization is essentially independent of the magnetic state [26], or (ii) the giant magneto-elastic coupling found by Lee *et al* [7].

5. The magneto-electric coupling tensor

From the above calculations one should be able to extract the linear magneto-electric tensor α. Indeed, in the magnetic phase, as soon as one is a little away from the transition temperature, the free energy is dominated by the magnetic energy and one can safely assume that

$$\alpha = -\frac{\partial^2 \mathcal{F}}{\partial \vec{\mathcal{E}} \partial \vec{\mathcal{H}}}\bigg|_{\substack{\mathcal{E}=\vec{0} \\ \mathcal{H}=\vec{0}}} = \sum_{\vec{R}} \sum_{\langle i,j \rangle} \frac{\partial^2 J_{ij} \langle \vec{S}_i \cdot \vec{S}_j \rangle}{\partial \vec{\mathcal{E}}\, \partial \vec{\mathcal{H}}}$$
$$\simeq \sum_{\vec{R}} \sum_{\langle i,j \rangle} \frac{\partial J_{i,j}}{\partial \vec{\mathcal{E}}} \cdot \left(\frac{\partial \langle \vec{S}_i \rangle}{\partial \vec{\mathcal{H}}} \cdot \langle \vec{S}_j \rangle + \langle \vec{S}_i \rangle \cdot \frac{\partial \langle \vec{S}_i \rangle}{\partial \vec{\mathcal{H}}} \right).$$

The present *ab initio* calculations gave us the $\frac{\partial J_{i,j}}{\partial \vec{\mathcal{E}}}$ factors. For the $\frac{\partial \langle \vec{S}_i \rangle}{\partial \vec{\mathcal{H}}}$ one, the Mn^{3+} ions being $S = 2$ can be treated as classical spins and the solution of the Heisenberg Hamiltonian under a magnetic field derived for the 2D triangular lattice associated with each layer. Labeling each of the three sublattices λ, μ, ν one gets for the $z = 0$ layer

$$\alpha_{z=0} = \frac{\mu_0 \mu_B}{3J} S \left\{ \frac{\partial J_{\lambda,\mu}}{\partial \vec{\mathcal{E}}} \otimes \begin{pmatrix} \frac{3\sqrt{3}}{2} \\ \frac{3}{2} \\ 0 \end{pmatrix} + \frac{\partial J_{\mu,\nu}}{\partial \vec{\mathcal{E}}} \begin{pmatrix} 0 \\ -3 \\ 0 \end{pmatrix} \right.$$
$$\left. + \frac{\partial J_{\nu,\lambda}}{\partial \vec{\mathcal{E}}} \begin{pmatrix} \frac{\sqrt{3}}{2} \\ \frac{3}{2} \\ 0 \end{pmatrix} \right\}$$

where S is the norm of the atomic spins. Applying now the symmetry operations relating the $z = 0$ and the $z = 1/2$ layers, one gets $\frac{\partial J_{i,j}(z=0)}{\partial \vec{\mathcal{E}}} = -\frac{\partial J_{i,j}(z=1/2)}{\partial \vec{\mathcal{E}}}$ and thus

$$\alpha = \begin{pmatrix} 0 & 0 & 0 \\ 0 & 0 & 0 \\ 0 & 0 & 0 \end{pmatrix}.$$

This conclusion should be put in perspective with experimental data. Indeed, the measurement of the dielectric constant as a function of the temperature does not exhibit any divergence [9], as should be the case, according to Landau analysis, for a linear magneto-electric coupling; that is α must be null as we found from symmetry analysis.

6. Conclusion

We computed, using a combination of different first principle methods, the evolution of the magnetic exchange integrals as a function of an applied electric field. For this purpose a specific procedure was designed, combining DFT calculations for the degrees of freedom related to the whole electronic density (polarization, Born charge tensor, Hessian matrix), and embedded fragment, explicitly correlated, quantum chemical calculations for the degrees of freedom related to the strongly correlated Fermi electrons (magnetic couplings). One should notice that this method was able to reach experimental accuracy on the magnetic couplings without any adjustable parameter.

Our calculations allowed us to investigate the relative importance of the exchange-striction and of the spin–orbit effects. We found that, in this system, the Dzyaloshinskii–Moriya contribution to the magneto-electric effect remains about two orders of magnitude weaker than the exchange-strictive contribution. These results support previous hypotheses proposed from the observation of a giant magneto-elastic effect [7], and from the insensitivity of DFT polarization calculations to the magnetic ordering [26]. Another important conclusion for the experimentalists comes from the weakness of the magnetic exchange variation, under applied electric field of experimentally accessible amplitude.

Finally, knowing the dependence of the exchange integrals on applied electric field, one can compute the linear magneto-electric coupling tensor. Our calculations however showed that this tensor is null, due to the symmetry operations relating the two magnetic layers belonging to the unit cell along the **c** direction.

$YMnO_3$ is a type I multiferroic compound; that is, the magnetic and ferroelectric transitions are not directly coupled. For type II multiferroic systems this is not the case, and the spin–orbit interaction is usually assumed to be responsible for the magneto-electric coupling [30]. It would thus be of great interest to perform such calculations for a type II compound in order to clarify the role and relative importance of the magnetostrictive–electrostrictive and spin–orbit interactions.

Acknowledgments

The authors thank D Maynau and V Vallet for providing us with the CASDI and EPCISO packages, and Ch Simon and K Singh for helpful discussions. This work was done with the support of the French national computer center IDRIS under project no 081842 and the regional computer center CRIHAN under project no 2007013.

References

[1] Curie P 1894 *J. Physique* **3** 393
[2] Bauer E 1926 *C. R. Acad. Sci.* **182** 1541
[3] Kimura T, Goto T, Shintanl H, Ishizaka K, Arima T and Tokura Y 2003 *Nature* **426** 55
Goto T, Kimura T, Lawes G, Ramirez A P and Tokura Y 2004 *Phys. Rev. Lett.* **92** 257201
Hur N, Park S, Sharma P A, Ahn J S, Guha S and Cheong S W 2004 *Nature* **429** 392
[4] Huang Z K, Cao Y, Sun Y Y, Xue Y Y and Chu C W 1997 *Phys. Rev.* B **56** 2623
Katsufuji T, Mori S, Masaki M, Moritomo Y, Yamamoto N and Takagi H 2001 *Phys. Rev.* B **64** 104419
[5] Goltsev A V, Pisarev R V, Lottermoser Th and Fiebig M 2003 *Phys. Rev. Lett.* **90** 177204
[6] Hanamura E and Tanabe Y 2003 *J. Phys. Soc. Japan* **72** 1959
[7] Lee S *et al* 2008 *Nature* **451** 805
[8] Lee S, Pirogov A, Han J H, Park J-G, Hoshikawa A and Kamiyama T 2005 *Phys. Rev.* B **71** 184413

[9] Singh K, Lepetit M-B, Simon Ch, Bellido N, Varignon J, Pailhès S and De Muer A 2013 *J. Phys.: Condens. Matter* **25** 416002
[10] Bertaud E F, Pauthenet R and Mercier M 1963 *Phys. Lett.* **7** 110
Muñoz A, Alonso J A, Martínez-Lopez M J, Casaís M T, Martínez J L and Fernández-Díaz M T 2000 *Phys. Rev.* B **62** 9498
[11] Brown P J and Chatterji T 2006 *J. Phys.: Condens. Matter* **18** 10085
[12] Bousquet E, Spaldin N A and Delaney K T 2011 *Phys. Rev. Lett.* **106** 107202
[13] Mostovoy M, Scaramucci A, Spaldin N A and Delaney K T 2010 *Phys. Rev. Lett.* **105** 087202
[14] Gellé A, Varignon J and Lepetit M-B 2009 *Europhys. Lett.* **88** 37003
[15] Petit S, Moussa F, Hennion M, Pailhès S, Pinsard-Gaudart L and Ivanov A 2007 *Phys. Rev. Lett.* **99** 266604
[16] Park J, Park J-G, Jeon G S, Choi H-Y, Lee C, Jo W, Bewley R, McEwen K A and Perring T G 2003 *Phys. Rev.* B **68** 104426
[17] Moriya T 1960 *Phys. Rev.* **120** 91
[18] Iñiguez J 2008 *Phys. Rev. Lett.* **101** 117201
[19] Malashevich A, Coh S, Souza I and Vanderbilt D 2012 *Phys. Rev.* B **86** 094430
Scaramucci A, Bousquet E, Fechner M, Mostovoy M and Spaldin N A 2012 *Phys. Rev. Lett.* **109** 197203
[20] See for instance: Moreira I de P R, Illas F, Calzado C J, Sanz J F, Malrieu J-P, Ben Amor N and Maynau D 1999 *Phys. Rev.* B **59** R6593
Lepetit M B 2002 How to determine model Hamiltonians for strongly correlated materials *Recent Research Developments in Quantum Chemistry* vol 3 (Trivandrum: Transworld Research Network) p 143
Gellé A and Lepetit M-B 2005 *Eur. Phys. J.* B **46** 489
[21] Winter W, Pitzer R M and Temple D K 1987 *J. Chem. Phys.* **86** 3549
[22] Gellé A and Lepetit M-B 2008 *J. Chem. Phys.* **128** 244716
[23] Dovesi R, Orlando R, Civalleri B, Roetti C, Saunders V R and Zicovich-Wilson C M 2005 *Z. Kristallogr.* **220** 571
Dovesi R *et al* 2009 *CRYSTAL09 User's Manual* (Torino: University of Torino)
[24] Bilc D I, Orlando R, Shaltaf R, Rignanese G M, Iñiguez J and Ghosez P 2008 *Phys. Rev.* B **77** 165107
[25] Hay P J and Wadt W R 1985 *J. Chem. Phys.* **82** 299
Evarestov R A, Kotomin E A, Heifets E, Maier J and Borstel G 2003 *Solid State Commun.* **127** 367
Gellé A and Calzado C 2013 private communication
[26] Varignon J, Petit S and Lepetit M-B 2013 at press (arXiv:1203.1752 [cond-mat.str-el])
[27] Karlstöm G *et al* 2003 *Comput. Mater. Sci.* **28** 222
[28] Vallet V, Maron L, Teichteil C and Flament J P 2000 *J. Chem. Phys.* **113** 1391
[29] Barandiaran Z and Seijo L 1992 *Can. J. Chem.* **70** 409
Seijo L 2013 unpublished
[30] See for instance: Sergienko I A and Dagotto E 2006 *Phys. Rev.* B **73** 094434
Li Q, Dong S and Liu J M 2008 *Phys. Rev.* B **77** 054442
Shanavas K V, Choudhury D, Dasgupta I, Sharma S M and Sarma D D 2010 *Phys. Rev.* B **81** 212406